
CASE REPORT

Late-onset Urea Cycle Deficiency is an Under-recognised Cause of Metabolic Childhood Encephalopathy: a Case Report

C Tsoi¹, EKC Law¹, J Hui², WCW Chu¹

¹*Department of Imaging and Interventional Radiology, Prince of Wales Hospital, The Chinese University of Hong Kong, Hong Kong*

²*Department of Paediatrics, Prince of Wales Hospital, The Chinese University of Hong Kong, Hong Kong*

INTRODUCTION

Metabolic disorders of the brain can manifest at any age. During the neonatal period or early infancy they can be associated with acute and severe illness. Nonetheless due to the complex genotypic variability and penetrance, a subset of inborn errors of metabolism can manifest in late childhood or even adulthood. This often results in clinically confounding situations and diagnosis is difficult. We present the clinical and imaging findings in a 6-year-old girl with late-onset urea cycle defect. The patient initially presented with lethargy and confusion with signs of encephalopathy. Peripheral blood demonstrated an increased plasma ammonia level. Multiparametric magnetic resonance imaging (MRI) including diffusion-weighted sequence and spectroscopy provided clues to the diagnosis but the patient deteriorated quickly from neurotoxicity of the metabolites. A high index of clinical suspicion, together with biochemical profile and imaging assessment are required to ensure early initiation of appropriate treatment.

CASE REPORT

A 6-year-old Chinese girl presented to the accident and

emergency department in January 2016 with confusion and lethargy. She had a 2-day history of upper respiratory tract infection and fever. Physical examination revealed a child who was lethargic, disorientated in time and space, and unable to recognise her parents. Her medical history was unremarkable. She was born to healthy non-consanguineous parents, and her antenatal and postnatal history was unremarkable apart from a similar but milder episode of vomiting and lethargy 1 year earlier, which was attributed to influenza A infection, followed by an uneventful recovery. After admission to the paediatric intensive care unit she experienced a few episodes of seizures and status epilepticus. Lumbar puncture revealed normal biochemistry (cerebrospinal fluid glucose 6.2 mmol/L, lactate 2.9 mmol/L, protein 0.17 g/L, white blood cell $14 \times 10^6/L$) and was negative for both bacterial and viral infections on culture and polymerase chain reaction tests, respectively. Preliminary biochemistry investigations from blood tests revealed slightly raised lactate (4.4 mmol/L; normal range 0.7-2.1 mmol/L), a rising trend of ammonia (143.8-364 $\mu\text{mol/L}$ within 24 hours; normal $<48 \mu\text{mol/L}$) and respiratory alkalosis (pH 7.55).

Correspondence: Prof WCW Chu, Department of Imaging and Interventional Radiology, Prince of Wales Hospital, The Chinese University of Hong Kong, Hong Kong.

Email: winniechu@cuhk.edu.hk

Submitted: 12 Feb 2019; Accepted: 24 Mar 2020

Contributors: All authors designed the study and acquired the data. CT, EKCL, WCWC analysed the data, drafted the manuscript, and critically revised the manuscript for important intellectual content. All authors had full access to the data, contributed to the study, approved the final version for publication, and take responsibility for its accuracy and integrity.

Conflicts of Interest: All authors have disclosed no conflicts of interest.

Funding/Support: This research received no specific grant from any funding agency in the public, commercial, or not-for-profit sectors.

Data Availability: All data generated or analysed during the present study are available from the corresponding author on reasonable request.

Ethics approval: The patient was treated in accordance with the tenets of the Declaration of Helsinki. The patient provided written informed consent for all treatments and procedures.

Electroencephalography demonstrated diffuse slow background without normal sleep potential, suggestive of encephalopathy. Initial plain computed tomography (CT) scan of the brain on the day of presentation (Figure 1a) was unremarkable with preserved grey-white differentiation. MRI brain examination on the third day of presentation showed extensive T2 signal changes in both cerebral hemispheres, with restricted diffusion involving the cortical and subcortical regions and sparing the perirolandic region, occipital lobes, and caudate and lentiform nuclei (Figure 2). The dorsomedial thalami were also symmetrically involved. Follow-up plain CT scan of the brain (Figure 1b) at 1 day after MRI examination revealed marked cytotoxic oedema involving both cerebral hemispheres, in agreement with earlier MRI findings. Further metabolic screening showed a markedly raised plasma glutamine level $>1500 \mu\text{mol/L}$ (normal range, $254\text{--}823 \mu\text{mol/L}$) and prompted investigation for urea cycle defect. Further genetic tests of the *CPS1* gene identified a gene mutation of heterozygous *CPS1* c.2407C>G p.(Arg830G1y) and c.4088_4099delTGATAGGCATCC. P(Leu1363_Ile366del), likely pathogenic in nature. Compound heterozygosity of the two detected likely pathogenic variants was confirmed by parental genetic analysis. Results were consistent with a diagnosis of carbamoyl phosphate synthetase 1 deficiency.

In view of the diffuse cerebral oedema, craniectomy was performed to relieve the raised intracranial pressure. The patient was treated with intravenous sodium benzoate/phenylbutyrate infusion to suppress ammonia level

and commenced on a low protein, high calorie diet. Nonetheless subsequent assessment revealed poor neurological recovery and global developmental delay due to prolonged hyperammonaemic coma.

Follow-up MRI scan of the brain 6 months later showed profound diffuse cerebral atrophy and cystic encephalomalacia with residual white matter change as sequelae of the previous irreversible insult to bilateral frontal, anterior parietal and insular regions (Figure 3). Magnetic resonance (MR) spectroscopy was also performed on a 3T whole-body scanner (Achieva TX, Philips Healthcare) using a standard 8-channel head coil. With image guidance, MR spectroscopy was performed on a voxel positioned in the right parietal region of the brain using a PRESS (Point RESolved Spectroscopy) sequence (repetition/echo times, 2000/31 ms) with 128 signal averages. Automated second-order shimming and water suppression were applied prior to signal acquisition. MR spectroscopy data were exported and processed offline using LCModel software package (version 6.3) allowing an accurate measurement of the metabolites present in the subject. The short echo time spectrum showed a marked reduction in N-acetylaspartate (2.02 ppm) related to profound neuronal loss, and prominent lipid peaks at 0.9 and 1.3 ppm. The presence of lactate (1.32 ppm) could not be confirmed as the strong lipid signal at 1.3 ppm found in the spectrum made the detection of lactate more difficult. Both choline-containing compounds and glutamine signals were also elevated, compatible with accumulation of urea precursors (Figure 4).

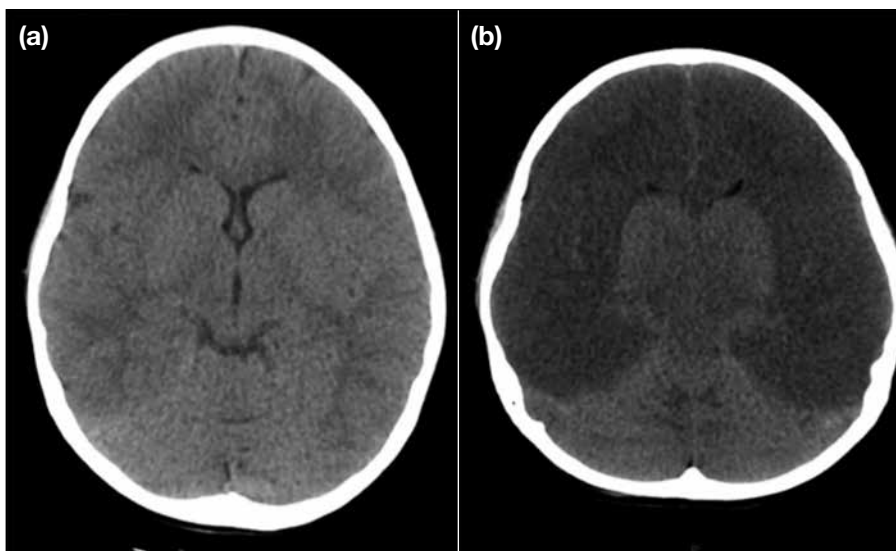


Figure 1. A 6-year-old Chinese girl presenting with confusion and lethargy. Plain computed tomography scans of the brain (a) on the day of presentation showing preserved grey-white differentiation, and (b) on day 4 of presentation showing dramatic interval changes with marked cerebral oedema and loss of grey-white differentiation sparing the caudate and lentiform nuclei.

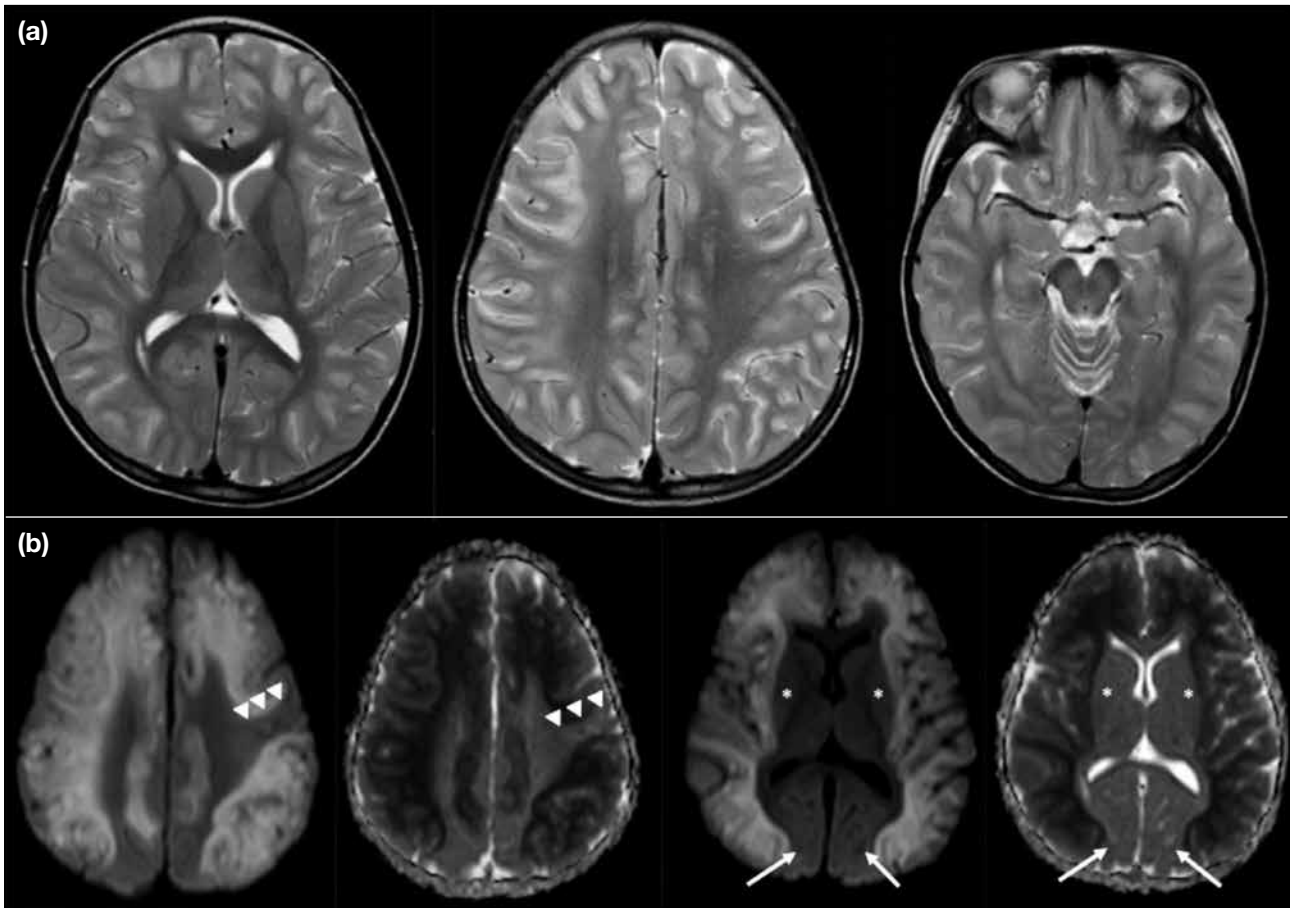


Figure 2. Same patient on day 3 after admission. (a) T2-weighted magnetic resonance (MR) images showing extensive cerebral oedema sparing the caudate and lentiform nuclei, occipital lobes, and periorlandic region. (b) Diffusion-weighted MR images and corresponding apparent diffusion coefficient maps at two levels showing extensive restricted diffusion in the corresponding area of cerebral oedema, sparing the caudate and lentiform nuclei (asterisks), occipital lobes (arrows), and periorlandic regions (arrowheads).

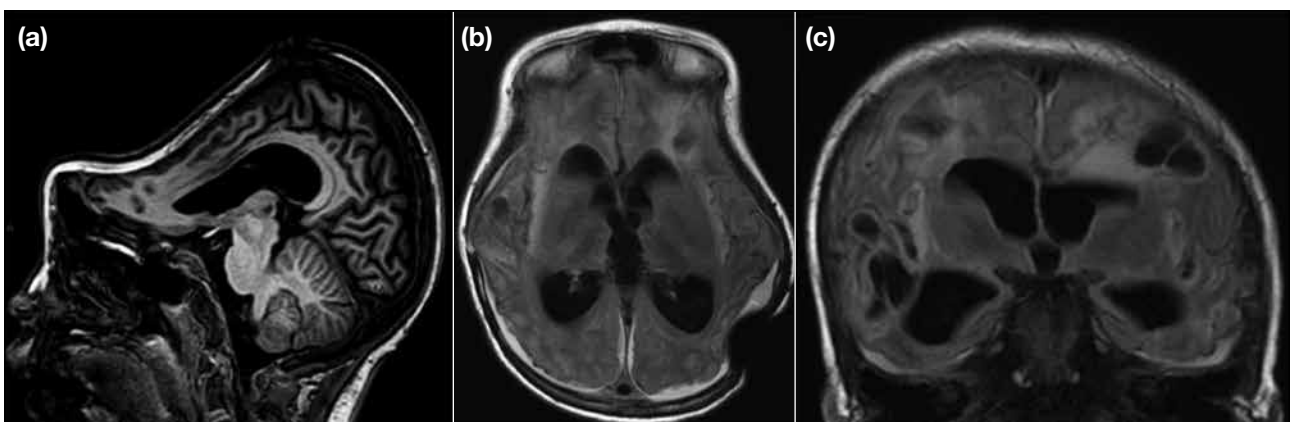


Figure 3. Same patient at 6 months after diagnosis. (a) Sagittal T1-weighted magnetic resonance (MR) image showing atrophic and deformed frontal lobe related to previous craniectomy. Fluid attenuated inversion recovery sequences (b) axial and (c) coronal MR images showing cystic encephalomalacia and residual white matter T2-hyperintensities in bilateral frontal, anterior parietal, and insular regions.

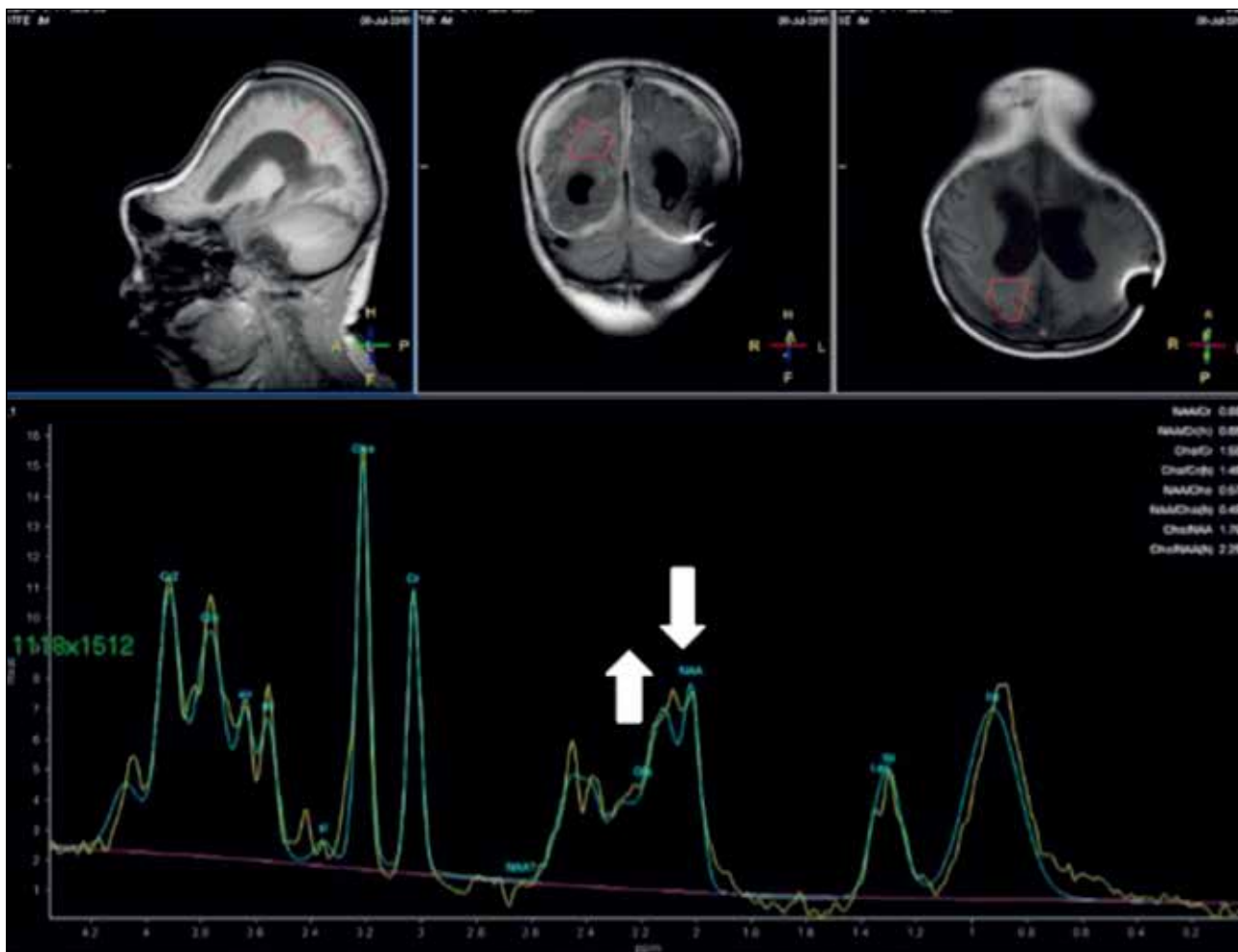


Figure 4. Same patient at 6 months after diagnosis. Magnetic resonance spectroscopy with regions of interest over right parietal white matter showing reduced N-acetylaspartate and raised glutamine and glutamate levels.

DISCUSSION

Childhood encephalopathy is a paediatric emergency and poses a considerable clinical challenge with a long list of differential diagnoses. It carries high morbidity and mortality. Prompt diagnosis and timely treatment can significantly minimise neurological sequelae in some cases. The presentation can be acute or insidious. A systematic approach is key to early diagnosis (Figure 5). In this case, hyperammonaemia was a hallmark for underlying inborn error of metabolism and urea cycle defect.

Urea cycle defect is a group of genetic disorders associated with deficiency in any one of the five enzymes involved in the urea cycle.¹ The collective prevalence of urea cycle defect is approximately 1 in 8000 live births. Urea cycle defect involves accumulation of urea

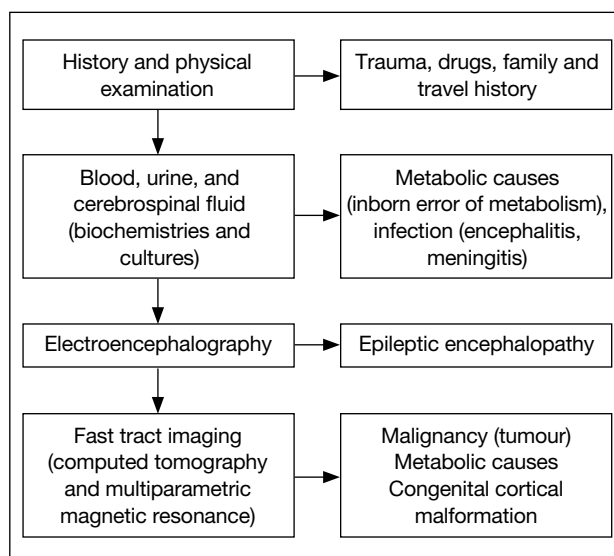


Figure 5. Diagnostic algorithm for childhood encephalopathy.

precursors such as ammonia and nitrogenic compounds such as glutamine. These chemicals accumulate rapidly in the brain as ammonia crosses the blood-brain barrier freely, with a direct consequence of neurotoxicity at a cellular level, or an indirect effect of glutamine synthesis that is osmotically active and often leads to cytotoxic oedema and consequent encephalopathy.² Most patients present with neurological symptoms. All defects in the urea cycle are recessively inherited except for the most common defect, ornithine transcarbamylase deficiency that is linked to the X-chromosome.¹

Patients with urea cycle defects present with a broad spectrum of symptoms due to variable residual enzyme activity. Hyperammonaemia crises that include non-specific symptoms such as loss of appetite, vomiting and seizures most commonly occur during the neonatal period. The timing of onset and severity depends on the nature of the molecular defect and the body's capacity to eliminate the toxic nitrogenic products.² Affected neonates often appear healthy for the initial 24 to 48 hours of life, then present with progressive lethargy, hypothermia, and apnoea. Late-onset patients usually have a milder form of enzyme defects and often present from infancy to adulthood with less acute symptoms such as chronic encephalopathy, learning disorders, and vomiting. Acute presentation as encephalopathy is often aggravated by a high protein intake and illness due to subsequent catabolism that exceeds the body's threshold to eliminate toxic precursors.²

As illustrated in the current case, our patient was a late presenter with insidious onset of symptoms. The metabolic defect was not detected at an early stage of clinical presentation, leading to a delay in diagnosis and irreversible and catastrophic neurological damage. It is worth noting that our patient had presented with a similar episode of lethargy and vomiting a year prior to the irreversible insult. The duration and degree of hyperammonaemia and coma may predict the prognosis and extent of neurological damage.² A high index of suspicion of a metabolic cause should always be maintained in cases of neurological derangement since early treatment may minimise or prevent neurologic sequelae by minimising protein catabolism and elimination of ammonia.

Neuroimaging plays an important role in the diagnostic process.

The initial apparently normal CT brain may have been

due to its lower sensitivity to detect acute changes.

From an imaging perspective, the imaging appearances of different enzyme deficiencies within the urea cycle defect are similar, likely due to similar metabolic derangements downstream in the cellular pathway. Hyperammonaemia and hyperglutaminaemia alter intracellular osmolality, resulting in brain oedema and intracranial hypertension, and finally secondary cerebral hypoperfusion.

Similar imaging findings and involvement have been described previously.^{3,4} Takanashi et al⁵ described five types of MR appearance in urea cycle defects, speculated to differ by their residual enzyme activity and clinical severity: (1) extensive diffuse severe cerebral oedema involving both grey and white matter, resembling hypoxic-ischaemic encephalopathy (HIE) in the subacute phase, followed by generalised atrophy, usually seen in survivors of severe deficiency with prolonged neonatal coma; (2) infarct-like appearance in a hemispheric fashion so patients can present with stroke-like events; (3) less severe ischaemic events in intervascular boundaries; (4) symmetrical cortical involvement of the cingulate gyri, temporal lobes, insular cortex with sparing of perirolandic cortex and occipital lobes in childhood or adult patients with partial deficiencies,^{3,4} and (5) preferential involvement of white matter of the brain, involving the lentiform nuclei, deep sulci of the insular and perirolandic regions in patients with neonatal presentation. These areas have highest metabolic activity at birth and are most susceptible to hypoperfusion in a hyperammonaemic state, reflected on MR images and contrast with different patterns of involvement in children and adults.⁵ In all cases, it is speculated that the imaging appearances are related to underlying hypoperfusion during hyperammonaemia.⁵ The extent of cerebral involvement and presence of diffusion restriction has a role in predicting the severity of neurological sequelae.⁶

Among them, type 4 pattern, which was seen in our case, has also been reported in patients with hyperammonaemia due to other causes such as valproic acid-induced hyperammonaemic encephalopathy and acute hepatic encephalopathy. This suggests that the appearance might be related to hyperammonaemia rather than the underlying disorder.⁴ This appearance probably represents a milder form of disease wherein the ischaemic insults may be partially reversible if promptly treated. Extensive cortical involvement on MRI (type 1 pattern) mimics severe HIE. Unlike HIE, the degree of

apparent diffusion coefficient reduction in urea cycle defects appears to be less severe and reversible to a certain degree.⁷

MR spectroscopy provides further information in terms of the biochemistry. MR spectroscopy appearances are consistent with the metabolic derangement and demonstrate elevated glutamine and decreased myoinositol and choline in severely affected patients.¹ It can also be used to monitor adequacy of metabolic control.

CONCLUSION

Recognition of a specific neuroimaging pattern together with a high index of clinical suspicion of late-onset urea cycle defect in patients who present with encephalopathy can guide further genetic tests specific for urea cycle defect. Early treatment may alleviate and minimise the devastating neurological sequelae.

REFERENCES

1. Patay Z. MR imaging workup of inborn errors of metabolism of early postnatal onset. *Magn Reson Imaging Clin N Am*. 2011;19:733-59.
2. Gropman AL, Summar M, Leonard JV. Neurological implications of urea cycle disorders. *J Inher Metab Dis*. 2007;30:865-79.
3. Bindu PS, Sinha S, Taly AB, Christopher R, Kover JM. Cranial MRI in acute hyperammonemic encephalopathy. *Pediatr Neurol*. 2009;41:139-42.
4. Takanashi JI, Barkovich AJ, Cheng SF, Kostiner D, Baker JC, Packman S. Brain MR imaging in acute hyperammonemic encephalopathy arising from late-onset ornithine transcarbamylase deficiency. *AJNR. Am J Neuroradiol*. 2003;24:390-3.
5. Takanashi JI, Barkovich AJ, Cheng SF, Weisiger K, Zlatunich CO, Mudge C, et al. Brain MR imaging in neonatal hyperammonemic encephalopathy resulting from proximal urea cycle disorders. *AJNR Am J Neuroradiol*. 2003;24:1184-7.
6. Bireley WR, Van Hove JL, Gallagher RC, Fenton LZ. Urea cycle disorders: brain MRI and neurological outcome. *Pediatr Radiol*. 2012;42:455-62.
7. Krishna SH, McKinney AM, Lucato LT. Congenital genetic inborn errors of metabolism presenting as an adult or persisting into adulthood: neuroimaging in the more common or recognizable disorders. *Semin Ultrasound CT MR*. 2014;35:160-91.